

**Infrared, Electronic,  
and Electron Spin Resonance Spectra  
of Pyridine-2,6-dithiocarbomethylamide  
Copper(II) Complexes\*\***

**Alois Popitsch<sup>a,\*</sup> and Rainer Czaputa<sup>b</sup>**

<sup>a</sup> Institut für anorganische Chemie, Universität Graz, A-8010 Graz, Austria

<sup>b</sup> Institut für Experimentalphysik, Universität Graz, A-8010 Graz, Austria

(Received 4 May 1983. Accepted 20 May 1983)

Copper(II) complexes of pyridine-2,6-dithiocarbomethylamide (*PDTA*) of the general formula  $\text{CuPDTA}\cdot X, L$  ( $X = \text{Cl}_2, \text{Br}_2, \text{I}_2, \text{NO}_3, \text{SO}_4, 2\text{HC}_2\text{O}_4, \text{H}_2\text{O}, \text{NH}_3$ , pyridine) have been prepared and characterized by elementary analysis, infrared-, electronic reflectance- and spin resonance- spectroscopy. The influence of the coordinated anions on the molecular stereochemistries is discussed on the basis of these data. The thermal behaviour of the complexes is described.

[*Keywords: Electronic spectra; Infrared spectra; Pyridine-2,6-dithiocarbomethylamide copper(II) complexes; Spin resonance spectra; Thermal analysis*]

*Infrarot-, optische und Elektronenspinresonanzspektren von Pyridin-2,6-dithiocarbomethylamid Kupfer(II)-Komplexen*

Kupfer(II)-Komplexe des Pyridin-2,6-dithiocarbomethylamids (*PDTA*) vom Typ  $\text{CuPDTA}\cdot X, L$  ( $X = \text{Cl}_2, \text{Br}_2, \text{I}_2, \text{NO}_3, \text{SO}_4, 2\text{HC}_2\text{O}_4, \text{H}_2\text{O}, \text{NH}_3$ , Pyridin) wurden hergestellt und analysiert. Über das thermische Verhalten dieser Verbindungen wird berichtet. Untersuchungen der Elektronenspinresonanz, Infrarot- und optischen Absorption geben Hinweise über den strukturechemischen Einfluß der koordinierten Anionen.

**Introduction**

Copper(II) displays a large number of coordination polyhedra, with coordination numbers four, five, and six being most common. The lack

\*\* Herrn Prof. Dr. *E. Schauenstein* zum 65. Geburtstag gewidmet.

of spherical symmetry of the copper(II) ion ( $3d^9$ ) is the major factor in the formation of non-regular stereochemistries. With certain limits the Cu(II) ion prolate ellipsoid is continuously variable and the term "plasticity" has been introduced to describe this non-rigid property. This behaviour was mainly studied on  $\text{CuO}_6$ ,  $\text{CuN}_6$ , and  $\text{CuN}_4\text{O}_2$  polyhedra<sup>1,2</sup>.

Copper(II) complexes of pyridine-2,6-dithiocarbomethylamide (PDTA) are suitable to investigate similar effects in molecular stereochemistries in which soft sulfur atoms influence the coordination sphere. The interest in the metal complexes derived from this tridentate chelate lies, beside its ability to form normal charged and neutral (inner) complexes by deprotonation of the thioamide groups, also in its potential possibility of N,S linkage isomerism<sup>3</sup>.

Recently the crystal structures of four copper complexes with this ligand have been determined<sup>4,5</sup>. Common to the three halide complexes is the square pyramidal chromophor  $\text{CuNS}_2\text{X}_2$ , depicted in Fig. 1.

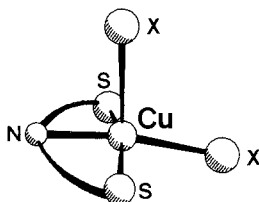


Fig. 1. The  $\text{CuPDTA-X}_2$  chromophor

In order to gain information on the influence of the associated anions on the  $\text{CuPDTA}$  moiety further complexes were synthesized. Their complementary physical properties (obtained from UV/VIS-, ESR-, IR- spectra and thermoanalytical data) are discussed in the present communication.

## Experimental

### Preparation

a)  $\text{CuPDTA-Py}$ . The complex was obtained by adding a methanolic solution of copper acetate (1 mol) to a solution of  $\text{PDTA}$  (1 mol) in methanol/pyridine (1:1). The crude neutral chelate was then recrystallized from chloroform. Thread-like needles formed upon cooling.

b)  $[(\text{CuPDTA})_x(\text{NH}_3)_x]$ . Procedure a) was repeated using gaseous ammonia instead of pyridine.

c)  $\text{CuPDTA-X, L}$ . The charged complexes were obtained by treating the neutral complex,  $\text{CuPDTA-Py}$ , with the appropriate acid (2N). Well formed green crystals were obtained. The analysis of the complexes are summarized in Table 1.

*Physical Measurements*

The diffuse reflectance spectra of the complexes were measured on a Cary 17 D instrument (absorbance readout; range 0–2.0; reference: magnesium carbonate).

The X-band ESR was carried out on powdered samples in the 5–300 K temperature range on a Bruker ER 200 D spectrometer equipped with a continuous flow cryostat and using *DPPH* ( $g = 2.0036$ ) as reference. To avoid orientation dependent powder spectra, the crystals were ground in a vibrating mill immersed in liquid nitrogen.

Infrared spectra were recorded on a Perkin-Elmer 580 B spectrometer at 300 and 80 K. Samples were prepared as CsI pellets and Nujol mulls on CsI plates.

Thermogravimetric analysis (TG) and differential thermal analysis (DTA) were performed on a Mettler TA2 instrument using micro Pt-cups. DTA peak areas were used to calculate enthalpies. The  $\Delta H$  value was estimated via the relation  $\Delta H = A \cdot K_a \cdot m^{-1}$  where  $A$  is the area,  $K_a$  is the calibration constant of the apparatus and  $m$  is the sample weight. The instrument was calibrated with standards in the conventional way, and the precision expected is around 5%<sup>6</sup>. The area under a peak was traced on high quality tracing paper, cut out and weighed. The experimental conditions for the DTA runs were as follows: heating rate: 2 °C/min, purge gas: dry nitrogen (100 ml/min), sample weights: ca. 10 mg; the crystals were covered with  $\alpha$ -Al<sub>2</sub>O<sub>3</sub>.

**Results and Discussion**

The analytical data given in Table 1 show that *PDTA* forms two types of copper complexes, viz., charged and neutral (deprotonated) complexes. For the former type X-ray structures<sup>4,5</sup> of the halide complexes show that the spatial arrangement of ligands around the copper ion is distorted square-based pyramidal with the halogen atoms occupying one basal and one apical site, and the metal atom displaced toward the fifth apical ligand by about 0.3 Å (the chromophore is depicted in Fig. 1). In contrast the crystal structure of the [Cu*PDTA*-H<sub>2</sub>O](NO<sub>3</sub>)<sub>2</sub>·H<sub>2</sub>O<sup>5</sup> shows a square coplanar stereochemistry with one water molecule as the fourth ligand. Square coplanar stereochemistries are very uncommon in Cu(II) complexes involving purely  $\sigma$ -bonding donor atoms, but do occur with potentially  $\pi$ -bonding ligands<sup>1</sup>. Although no crystal structure for the neutral Cu*PDTA*-*Pg* is available, the ESR spectral parameters give indirect evidence that the stereochemistry for this compound is entirely square coplanar (see below).

It is particularly interesting to compare physicochemical properties of a series of square based complexes with a spatially fixed CuNS<sub>2</sub>-skeleton, when crystal structure results are available for some of them. Such a comparison can provide information about the tendency of the remaining ligands (counter anions, solvated molecules) to stabilize certain stereochemistries.

Table 1. *Analysis, ESR, and electronic spectra of CuPDTA-X, L complexes*

Compound	C (%)		H (%)		N (%)		ESR spectra			Electronic spectra
	calc.	found	calc.	found	calc.	found	$g_1$	$g_2$	$g_3$	(kK)
[CuPDTA-Cl <sub>2</sub> ]H <sub>2</sub> O	28.6	28.6	3.5	3.5	11.1	11.0	2.040	2.056	2.173	13.3 (14.8)
[CuPDTA-Br <sub>2</sub> ]H <sub>2</sub> O	23.2	23.7	2.8	2.8	9.0	9.3	2.034	2.049	2.134	16.0 (15.4)
[CuPDTA-J <sub>2</sub> ]DMF	23.4	23.8	2.9	3.0	9.1	9.2		2.067		16.4; 13.5 (15.5)
[CuPDTA-H <sub>2</sub> O](NO <sub>3</sub> ) <sub>2</sub> ·H <sub>2</sub> O	24.1	24.1	3.3	3.5	15.6	15.8	2.057	2.152		17.1 (14.8)
[CuPDTA-NO <sub>3</sub> ](NO <sub>3</sub> )	26.2	25.9	2.7	2.6	17.0	16.8	2.036	2.060	2.179	16.3 (14.8)
[CuPDTA-SO <sub>4</sub> (H <sub>2</sub> O)]	26.8	27.0	3.2	3.4	10.4	10.8	2.027	2.065	2.188	ca.13.9 -
[CuPDTA-HC <sub>2</sub> O <sub>4</sub> (H <sub>2</sub> O)] <sub>2</sub> (C <sub>2</sub> O <sub>4</sub> )	32.8	32.5	3.2	3.1	9.6	9.5	2.030	2.067	2.188	ca.14.3 -
[(CuPDTA) <sub>x</sub> (NH <sub>3</sub> ) <sub>x</sub> ]	35.4	35.8	3.9	4.0	18.3	18.1	2.032	2.069	2.157	17.5 -
[CuPDTA-Py]	46.0	46.0	3.8	3.7	15.3	15.4		2.073		18.7; 14.3 (18.7)

### IR-Spectra

After elimination of the bands due to the polyatomic anions present, the spectra of the complexes in the mid-IR are very similar. Two examples are shown in Fig. 2 together with the free ligand. For the latter several bands have been assigned tentatively<sup>7</sup>. Upon complexation to a metal, the largest shift in frequency is found with vibrations involving the strongly coupled  $\nu_{\text{CN}}$ ,  $\nu_{\text{CS}}$ , and  $\delta_{\text{NH}}$  modes of the secondary thioamide groups [ $-\text{C}(\text{S})\text{NHCH}_3$ ]. Among them, the shift of the intense ligand band at  $1535\text{ cm}^{-1}$ , with mainly  $\nu_{\text{CN}}$  character, is most sensitive in distinguishing the donor atom of the side-chain. The frequency increase, as is found for the investigated complexes (to about  $1560\text{--}1600\text{ cm}^{-1}$ ), can be explained as resulting from a greater double bond character of the carbon—nitrogen bond on complexation through the thioamide sulfur atom. Further diagnostic informations about the coordination sphere are provided by copper—ligand stretching vibrations. In Table 2, tentatively assigned  $\nu_{\text{CuS}}$ ,  $\nu_{\text{CuN}}$ , and  $\nu_{\text{CuX}}$  frequencies are compared to the relevant interatomic distances.

The N—H stretching vibrations in the complexes are affected due to the vibrations in the extent and nature of hydrogen bonding in the complexes as compared to the free ligand. From the crystal structure of [CuPDTA-Br<sub>2</sub>]H<sub>2</sub>O<sup>5</sup>, for instance, it is known, that the thioamide hydrogen atom is linked to the solvated water molecule. Consequently, a further decrease in  $\nu_{\text{NH}}$  is observed, when the solvated molecule is removed thermochemically (cf. Fig. 2; PDTA:  $3300/3268$ ; [CuPDTA-Br<sub>2</sub>]H<sub>2</sub>O:  $3200$  and [CuPDTA-Br<sub>2</sub>]:  $3190/3070\text{ cm}^{-1}$ ). Stronger interaction of the type N—H...X<sup>-</sup> can be postulated for the deaquated complex and is also indicated by step 2 in the thermolyses (see below), where one HX is separated as part of the decomposition reaction.

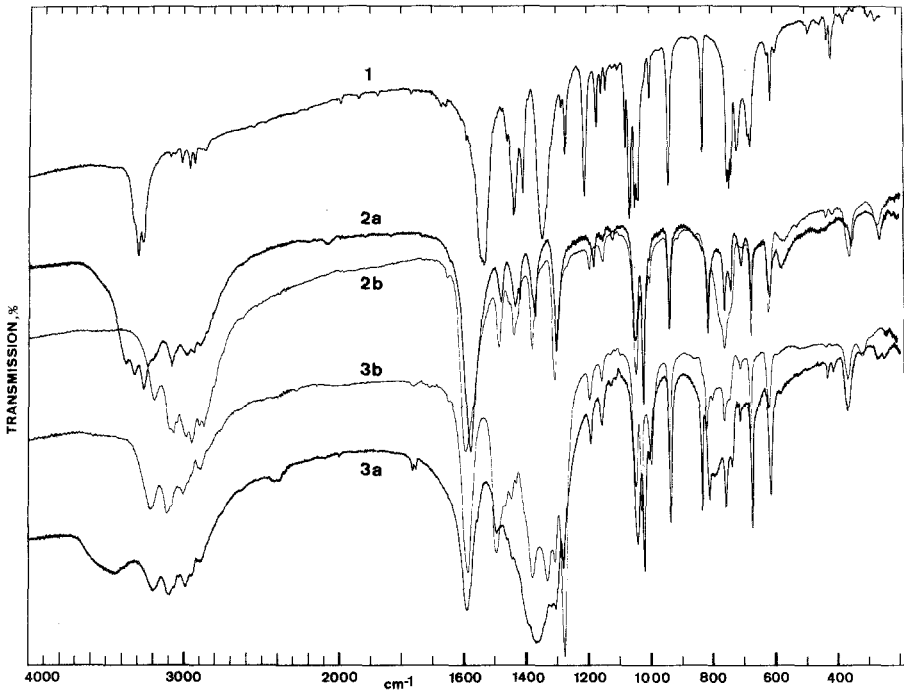


Fig. 2. Infrared spectra of: *PDTA* (1),  $[\text{CuPDTA}-\text{Br}_2]\text{H}_2\text{O}$  (2 a),  $[\text{CuPDTA}-\text{Br}_2]$  (2 b),  $[\text{CuPDTA}-\text{H}_2\text{O}](\text{NO}_3)_2 \cdot \text{H}_2\text{O}$  (3 a), and  $[\text{CuPDTA}-\text{NO}_3](\text{NO}_3)$  (3 b)

The most common means of establishing coordination of anions involve vibrational spectroscopy, where changes in the symmetry of the anion are reflected in the number and intensity of its fundamental vibrations.

The infrared spectrum of  $[\text{CuPDTA}-\text{H}_2\text{O}](\text{NO}_3)_2 \cdot \text{H}_2\text{O}$  shows a strong band at  $1345\text{ cm}^{-1}$  and a medium band at  $832\text{ cm}^{-1}$  assigned as the IR-allowed  $\nu_3$  and  $\nu_2$  modes, respectively, of the ionic nitrate group. The coordinated water molecule is clearly indicated (80 K spectrum) by bands at  $890\text{ cm}^{-1}$  ( $\rho_r(\text{H}_2\text{O})$ ),  $532\text{ cm}^{-1}$  ( $\rho_\omega(\text{H}_2\text{O})$ ) and  $465\text{ cm}^{-1}$  ( $\nu_{\text{Cu}-\text{OH}_2}$ ). Semi-coordination<sup>1</sup> of one  $\text{NO}_3^-$  ion and the second water molecule, vaguely indicated by weak bands at  $1400/1304$  ( $\nu_3, \text{NO}_3$ ),  $1770/1765$  ( $\nu_1 + \nu_2, \text{NO}_3$ ),  $782\text{ cm}^{-1}$  ( $\rho_r(\text{H}_2\text{O})$ ) and  $500\text{ cm}^{-1}$  ( $\rho_\omega(\text{H}_2\text{O})$ ), respectively, cannot be ruled out. These spectroscopic findings agree well with the reported crystal structure<sup>5</sup>.

In spite of its low position in the spectrochemical series, the nitrate ion was found to coordinate in a variety of environments. The  $\text{D}_{3h}$

Table 2. *Copper-ligand distances ( $\text{\AA}$ ) and stretching frequencies ( $\text{cm}^{-1}$ ) for some  $\text{CuPDTA-X, L}$  complexes*

Distance	$[\text{CuPDTA-Cl}_2]\text{H}_2\text{O}$		$[\text{CuPDTA-Br}_2]\text{H}_2\text{O}$		$[\text{CuPDTA-J}_2]\text{DMF}$		$[\text{CuPDTA-H}_2\text{O}](\text{NO}_3)\cdot\text{H}_2\text{O}$	
Mode								
Cu-S	2.291	2.297	2.284	2.287	2.279	2.279	2.250	2.307
$\nu(\text{Cu-S})$	342		348		352		365	
Cu-N	2.002		2.000		2.017		1.945	
$\nu(\text{Cu-N})$	265		265		238		266	
Cu-X	2.246	2.590	2.388	2.732	2.590	2.958	1.960	2.760
$\nu(\text{Cu-X})$	313		230/217		183/172		464	

symmetry of the ionic nitrate is lowered to  $\text{C}_{2v}$  for a linear monodentate or bidentate coordination and to  $\text{C}_s$  for a non-linear coordination.

The deaquated  $[\text{CuPDTA-NO}_3](\text{NO}_3)$ , obtained on heating the above compound to about  $150^\circ\text{C}$ , exhibit bands at  $1492 \text{ vs } (\nu_4)$ ,  $1276 \text{ vs } (\nu_1)$ ,  $993 \text{ s } (\nu_2)$ ,  $798 \text{ m } (\nu_6)$  and  $310 \text{ s cm}^{-1} (\nu_{\text{Cu-O}})$  which are characteristic of the bidentate nitrate group ( $\text{C}_{2v}$ -symmetry; cf. Fig. 2). The difference between the  $\nu_1$  and  $\nu_4$  frequencies has been used<sup>8</sup> as a guide to the covalent nature of the nitrate group: the greater the difference, the more covalent is the bonding. And a large value of  $\nu_4 - \nu_1$  (about  $200 \text{ cm}^{-1}$ ) is also indicative of bidentate nitrate. Additional splitting in the  $1400\text{--}1300 \text{ cm}^{-1}$  region indicate, that also the second nitrate may be slightly distorted due to weak coordination.

$[\text{CuPDTA-SO}_4(\text{H}_2\text{O})]$ . The multiplicity of the bands observed in the region anticipated for  $\text{C}_{2v}$  symmetry of the sulfate group with its degeneracy removed, viz.  $\nu_1$  (925),  $\nu_2$  (425),  $\nu_3$  as triplet (1030, 1173, and 1255) and  $\nu_4$  (605 and  $652 \text{ cm}^{-1}$ ), as well as the  $\text{Cu-O}$  stretching frequency at  $308 \text{ cm}^{-1}$ , suggest a chelating or a bridging bidentate sulfato complex<sup>8</sup>. A rhombic-octahedral stereochemistry can be assumed, since a coordinated water molecule is indicated by bands at  $860 \rho_r(\text{H}_2\text{O})$ ,  $505 \rho_w(\text{H}_2\text{O})$ , and  $440 \text{ cm}^{-1} \nu_{\text{Cu-OH}_2}$ .

The structure of complexes containing coordinated oxalate ligands is difficult to deduce from their infrared spectra alone. The oxalato group may act as a chelating or bridging ligand in different ways. The splitting in the  $\text{CO}$  stretching region ( $1800\text{--}1200 \text{ cm}^{-1}$ ) was found<sup>8,9</sup> to be a useful aid in distinguishing the different structures of this anion. In  $[\text{CuPDTA-HC}_2\text{O}_4(\text{H}_2\text{O})]_2(\text{C}_2\text{O}_4)$  the bands at  $1765 \text{ w}$ ,  $1685 \text{ w}$ ,  $1660 \text{ m}$ ,  $1210 \text{ m}$ , and  $789 \text{ m cm}^{-1}$  are assigned<sup>8,9</sup> to the unidentate anion; whereas bands at  $1715 \text{ m}$ ,  $1700 \text{ w}$ ,  $1628 \text{ vs}$ ,  $1435 \text{ m}$ , and  $1230 \text{ m cm}^{-1}$  indicate a bridging bidentate moiety. The frequencies at  $860 \text{ w}$ ,  $555 \text{ w}$ ,

and  $482\text{ m}/450\text{ m cm}^{-1}$  are attributed to coordinated water. Taken together, the infrared, electronic, and ESR spectra (see below) a binuclear rhombic-octahedral stereochemistry is suggested for this complex.

The greenish brown  $[(\text{CuPDTA})_x(\text{NH}_3)_x]$  is insofar different from the charged complexes and  $\text{CuPDTA-Py}$ , as additional strong ligand bands, viz. at  $1503$ ,  $1090$ , and  $1000\text{ cm}^{-1}$  indicate, that also one of the two thioamide nitrogen atoms is involved in coordination. A polymer two-dimensional structure with a coplanar  $\text{CuN}_2\text{S}_2$  chromophore is most probable, with the second sulfur atom coming from an adjacent  $\text{CuPDTA}$  moiety. The polymer structure is also supported by the low solubility of this compound in common polar or non polar solvents.

Weakly coordinated ammonia is indicated by bands at:  $3310\text{--}3100\text{ v}_s$ ,  $\text{v}_{as}(\text{NH}_3)$ ,  $1608\text{ }\delta_a(\text{HNH})$ ,  $1242\text{ }\delta_s(\text{HNH})$ ,  $648\text{ }\rho_r(\text{NH}_3)$ , and  $502/445\text{ cm}^{-1}\text{ v}_{\text{Cu-NH}_3}$ <sup>8,10</sup>. These bands disappear after heating the complex beyond  $170^\circ\text{C}$ , whereupon the ammonia molecule is split off.

#### *Magnetic Properties*

The magnetic moments and their temperature dependence between  $300$  and  $80\text{ K}$  of a number of  $\text{CuPDTA-X}$  complexes have been reported previously<sup>4</sup>. The room temperature magnetic moments lie within the range normally found in copper(II) complexes ( $\mu_{\text{eff}} 1.75\text{--}1.87\text{ B.M.}$ ), indicating magnetically dilute systems with orbitally non-degenerate states<sup>1</sup>.

#### *ESR Spectra*

The observed  $g$ -tensor parameters, obtained from the spectra of the polycrystalline samples, are listed in Table 1. The corresponding spectral line-shapes (first derivative) are depicted in Figs. 3, 4, and 5. The predominantly rhombic spectra show evidence of inhomogeneous broadening, which may slightly reduce the accuracy of the  $g$ -values. After grinding, no hyperfine splitting in the powdered spectra could be observed. In agreement with the magnetic data the intensities obey Curie's law for all complexes.

The order of the  $g$ -values ( $g_2 = g_{\parallel} > g_{\perp} > g_e$  or  $g_3 > g_2 > g_1 > g_e$ ) and their magnitudes suggest a dominant influence of the covalently bonded sulfur and nitrogen atoms. The values of the lowest  $g$ -factors in the anisotropic spectra ( $g_1$  range:  $2.027\text{--}2.067$ ) indicate a  $d_{x^2-y^2}$  ground state, consistent with (among other) square based pyramidal stereochemistries. It is well known<sup>1</sup> that exchange coupling cannot be ruled out if  $G < 4.0$  (where  $G = (g_{\parallel} - 2)/(g_{\perp} - 2)$ , with  $g_{\parallel} = g_3$  and  $g_{\perp} = (g_1 + g_2)/2$ ); This situation applies to the complexes under consideration.

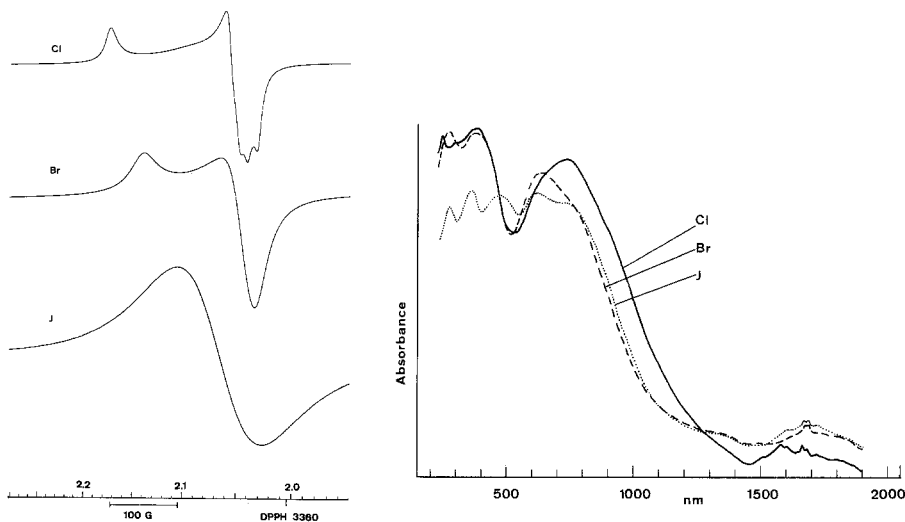


Fig. 3. ESR spectra (left) and electronic diffuse reflectance spectra (right) of:  $[\text{CuPDTA-Cl}_2]\text{H}_2\text{O}\cdots\text{Cl}$ ,  $[\text{CuPDTA-Br}_2]\text{H}_2\text{O}\cdots\text{Br}$ ,  $[\text{CuPDTA-I}_2]\text{DMF}\cdots\text{I}$

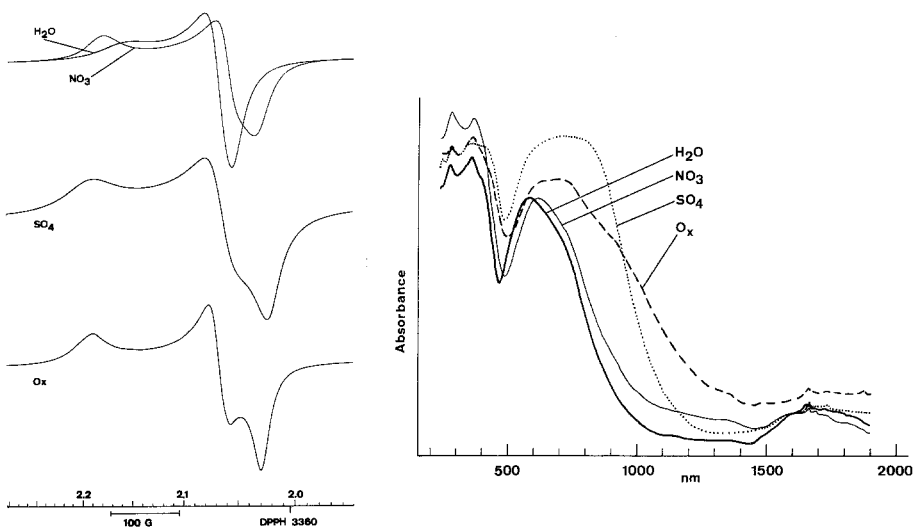


Fig. 4. ESR spectra (left) and electronic diffuse reflectance spectra (right) of:  $[\text{CuPDTA-H}_2\text{O}](\text{NO}_3)\cdot\text{H}_2\text{O}\cdots\text{H}_2\text{O}$ ,  $[\text{CuPDTA-NO}_3](\text{NO}_3)\cdots\text{NO}_3$ ,  $[\text{CuPDTA-SO}_4(\text{H}_2\text{O})]\cdots\text{SO}_4$ ,  $[\text{CuPDTA-HC}_2\text{O}_4(\text{H}_2\text{O})_2(\text{C}_2\text{O}_4)\cdots\text{O}_x$



The variation in the  $g_3 = g_{||}$  values may be explained by the influence of the ligand in axial position. As  $g_3$  decreases, this bond becomes more "covalent". Especially the decrease for the halide complexes follows the nephelauxetic series and the electronegativities of the coordinated atoms (cf. Fig. 3 and Table 1).

Preliminary single crystal ESR measurements for  $[\text{CuPDTA-Cl}_2]\text{H}_2\text{O}$  and the isomorphous  $[\text{CuPDTA-Br}_2]\text{H}_2\text{O}$  clearly show two magnetically nonequivalent sites, in agreement with their crystal structures<sup>4, 5</sup>, where pairs of antiparallel molecules ( $Z = 4$ ) related by an inversion center were observed in the unit cell. Despite careful grinding, orientation independent splitting of  $g_1$  is observed in the powder spectrum of  $[\text{CuPDTA-Cl}_2]\text{H}_2\text{O}$  (Fig. 3). No explanation for this behaviour could be obtained from the crystal structure. Preliminary single crystal measurements on  $[\text{CuPDTA-I}_2]\text{DMF}$  also show spectra consisting of three  $g$ -values. Therefore, the isotropic powder spectrum (Fig. 3) could be a consequence of appreciable exchange coupling, which reduces the spread of the  $g$ -values.

Fig. 5 shows the nearly isotropic ESR spectrum of the polycrystalline  $\text{CuPDTA-Py}$  (a), together with the first (b) and the second (c) deviation spectrum of this complex in benzene solution (room temper-

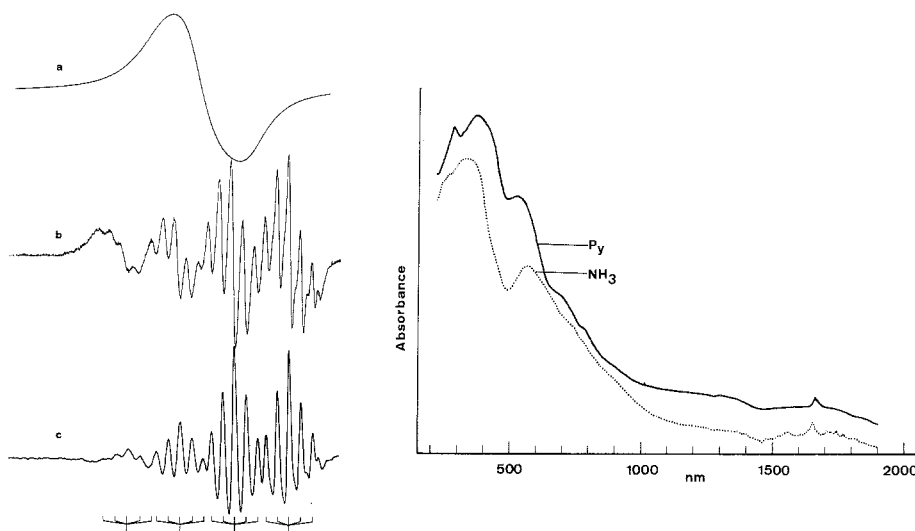


Fig. 5. ESR spectra (left) of  $[\text{CuPDTA-Py}]$ : (a) powder spectrum, (b) first-derivative, and (c) second-derivative ESR spectrum of the complex in benzene solution. Diffuse reflectance spectra (right) of  $[\text{CuPDTA-Py}] \cdots \text{Py}$  and  $[(\text{CuPDTA})_x \text{NH}_3]_x \cdots \text{NH}_3$

ature). As a result of motional narrowing, the solution spectra are characterized by the presence of three types of splitting: the hyperfine splitting ( $g_0 = 2.063$ ,  $A_{\text{Cu}} = 79.5 \cdot 10^{-4} \text{ cm}^{-1}$ ), caused by the interaction of the unpaired electron with the nuclear magnetic moment of copper ( $I = 3/2$ ); the superhyperfine splitting, which is due to strong interaction of the unpaired electron with the two nearly equivalent nitrogen nuclei ( $^{14}\text{N}$ ,  $I = 1$ ,  $A_{\text{N}} = 17.0 \cdot 10^{-4} \text{ cm}^{-1}$ ), yielding a well resolved five-line structure (intensity ratio of 1 : 2 : 3 : 2 : 1). The splitting excludes a coordination via thioamide nitrogen atoms and indicates a monomer species in solution. The magnitude of this splitting is close to values reported for a number of copper chelates with  $\alpha$ -thiopicoline anilides<sup>11</sup>. The third type of splitting is due to the isotopes  $^{65}\text{Cu}$  and  $^{63}\text{Cu}$  (with the same spin but somewhat different moments); it is particularly evident in the second deviation spectrum on the high field side. The planarity of the chelate is supported by the isotropic ESR spectra observed for both, the crystalline and the dissolved  $\text{CuPDTA-Py}$  complex.

### Electronic Spectra

The diffuse reflectance spectra are presented in Figs. 3, 4, and 5. As expected for  $3d^9$ -configuration, the spectra show a simple structure. They are similar, consisting of a broad maximum in the range 13.5–18.7 kK with the indication of a shoulder towards low energy. The  $d \rightarrow d$  transition maxima of the reflectance spectra are listed in Table 1, together with their shifts in ethanolic solution.

The small, but significant differences in the band maxima of the charged complexes in solution and their similar molar extinction coefficients ( $\epsilon$ -range: 300–450  $\text{l cm}^{-1} \text{ mole}^{-1}$ ) indicate, that the solid state structures are not preserved in solution. This supports the assumption that acido complexes of the type  $[\text{CuPDTA-X}, L_2]^+$  exist ( $L = \text{C}_2\text{H}_5\text{OH}$ ), as was previously inferred from conductance measurements for  $[\text{CuPDTA-Cl}_2]\text{H}_2\text{O}^3$ .

The solution spectrum of the neutral  $\text{CuPDTA-Py}$ , however, resembles the reflectance spectrum, indicating that the molecular structure is not affected by the solvent. This is also supported by the ESR results.

The spread in the  $d \rightarrow d$  band energies of the reflectance spectra [between 13.3 kK for  $[\text{CuPDTA-Cl}_2]\text{H}_2\text{O}$  (square pyramidal copper environment<sup>4</sup>) and 18.7 kK for  $\text{CuPDTA-Py}$  (effectively square-coplanar microsymmetry)] indicates a range of slightly different stereochemistries caused by the steric requirements of the coordinated anions and by their different  $\pi$ -bonding abilities. As the tetragonal

distortion increases from a tetrahedral stereochemistry towards a square-coplanar one, the centre of gravity of the  $d \rightarrow d$  transitions move towards higher energies. The differences in the ESR spectra suggest that the reflectance spectra are not resolved well enough to distinguish small structural differences.

Without polarized single-crystal spectra, a detailed ordering of one-electron energy levels cannot be discussed, but it was stated<sup>1</sup> that for a given stereochemistry the sequence of one-electron orbitals is essentially constant.

### Thermoanalysis

Data from TG and DTA curves are summarized in Table 3. As representative examples for the thermal behaviour of the  $\text{CuPDTA-X,L}$  complexes, Fig. 6 shows the TG and DTA curves for  $[\text{CuPDTA-Br}_2]\text{H}_2\text{O}$

Table 3. *The thermal decomposition of CuPDTA-X,L complexes*

Compound	step 1				step 2			
	$T_{\text{max}}$ (°C)	DTA $\text{kJmol}^{-1}$	Loss of weight (%)		Temp. range (T/°C)	Loss of weight (%)		
		calc.	found	calc.		found		
PDTA					169.2 (m.p.)			
$[\text{CuPDTA-Cl}_2]\text{H}_2\text{O}$	177	51	4.8	4.7	240-325	endo,exo	39.9	39.9
$[\text{CuPDTA-Br}_2]\text{H}_2\text{O}$	130	53	3.9	4.1	270-350	endo,exo	41.9	41.1
$[\text{CuPDTA-J}_2]\text{DMF}$	112	56	11.9	11.7	240-350	endo,exo	43.3	43.4
$[\text{CuPDTA-H}_2\text{O}](\text{NO}_3)_2 \cdot \text{H}_2\text{O}$	70	108	8.0	8.9	176-290	exo	-	62.0
$[\text{CuPDTA-SO}_4(\text{H}_2\text{O})]$	160	62	4.5	4.5	204-300	endo,exo	-	69.4
$[\text{CuPDTA-HC}_2\text{O}_4(\text{H}_2\text{O})]_2(\text{C}_2\text{O}_4)$	90	60	2.6	3.4	150	exo, 200-320	exo	- 55.0
$\{(\text{CuPDTA})_x\text{-(NH}_3)_x\}$	164	-	5.6	5.3	202-320	exo	-	37.9
$[\text{CuPDTA-Py}]$	202	-	21.6	21.6	215-320	exo	-	36.2

and  $[\text{CuPDTA-H}_2\text{O}](\text{NO}_3)_2 \cdot \text{H}_2\text{O}$ . It appeared interesting to investigate the dependence of the course of thermal decomposition on the different copper(II) coordination polyhedra.

The TG curves reveal essentially two-stage processes in the temperature range 25–400 °C, with the oxalato complex as the only exception. For the endothermic step 1, Table 3 gives the DTA peak temperature ( $T_{\text{max}}$ ), the decomposition enthalpy and the calculated and observed mass-loss percentages.

There are several ways in which solvated molecules can be incorporated in the crystal e.g., linked via hydrogen bonds to counter anions, incorporated as lattice solvate or coordinated to the central metal

atom. The former type was found in the crystal structure of the halogeno complexes<sup>4,5</sup>, the latter is present in  $[\text{CuPDTA}\cdot\text{H}_2\text{O}](\text{NO}_3)_2\cdot\text{H}_2\text{O}$ .

Deaquation of the  $[\text{CuPDTA}\cdot\text{H}_2\text{O}](\text{NO}_3)_2\cdot\text{H}_2\text{O}$  complex occurs between 55 and 85 °C in a single endothermic step ( $\Delta H = 54 \text{ kJ mol}^{-1}$  per  $\text{H}_2\text{O}$  released), although the crystal structure reveals considerably shorter bond length for  $\text{Cu}\text{---}\text{OH}_2$  in the equatorial plane (1.960 Å) than

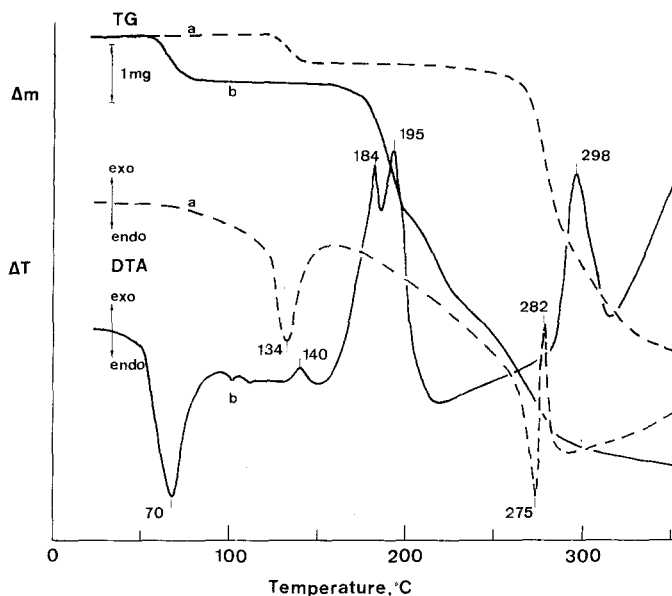


Fig. 6. Thermograms of (a)  $[\text{CuPDTA}\text{-Br}_2]\cdot\text{H}_2\text{O}$  and (b)  $[\text{CuPDTA}\text{-H}_2\text{O}](\text{NO}_3)_2\cdot\text{H}_2\text{O}$

for the water in the axial position (2.760 Å). The exotherm with a peak at 140 °C is interpreted as reorganization (partial substitution of the water molecules by nitrate ions) of the amorphous system into a crystalline phase (cf. DTA-trace in Fig. 6 b).

The decrease in  $T_{max}$  (Table 3) going from the chloro to the isomorphous bromo complex can be explained by the smaller ionic radius (and hence a higher electrostatic field for the  $\text{Cl}^-$  anion), leading to stronger  $\text{HOH}\cdots\text{X}^-$  bonds in the former compound.

A comparison of the decomposition temperatures and the deaqua-tion enthalpies for step 1 reveals that the differences do not allow any conclusions concerning the type of bond or its strength for the solvent molecules from TG/DTA measurements alone.

In the oxalato complex, exothermic degradation of the anion is observed at 150 °C. Three carbon monoxide equivalents are lost, yielding a carbonato complex as a stable intermediate.

The following, well-separated step 2 for the deaquated compounds does not reflect a simple one-stage process. Only the overall temperature regions and their mass-loss percentages are therefore listed in Table 3.

The DTA curves start with a narrow endotherm (melting endotherm?), immediately followed by an exotherm. The fine details in the DTG curves (not included in Fig. 6) indicate occasionally two- or three-stage degradation, without any well-defined plateau. The *pH* control of the released gaseous products indicate the initial elimination of an acidic molecule (HX). The following, obviously reductive [Cu(II)-Cu(I)] degradation is completed at about 330 °C in dynamic nitrogen atmosphere. Polymer residues of the empirical formula  $[\text{CuX}(\text{SCN})_2]_x$  are indicated by the calculated weight-losses for the halo-complexes (cf. Table 3) and confirmed by infrared spectra. Roughly the same formula can be calculated for the complex with polyatomic anions.

Comparing the initial decomposition temperatures of step 2 for the *CuPDTA-X,L* complexes with one another, it is evident that there are considerable influences of the anions. The halogeno complexes are most stable, with bromo more stable than chloro. The reduced stability for complexes with polyatomic anions could be a consequence of stronger Cu—S bonds with concomitant strengthening of the thioamide C—N bonds (compare also the  $\nu_{\text{CuS}}$  frequencies in Table 2). The electronic shift  $\text{N}^{\ominus}=\text{C}=\text{S}^{\ominus} \rightarrow \text{M}$  would weaken the adjacent C—C and N—CH<sub>3</sub> bonds, and the decomposition in step 2 would result in the residue  $[\text{CuX}(\text{SCN}_2)]_x$ .

### Conclusion

According to the electronic spectra and magnetic data, there is a continuous transition between square coplanar and octahedral stereochemistry in the complexes studied.  $\pi$ -electron acceptor ligands (pyridine) stabilize the former, polarisable ligands ( $\pi$ -electron donor ligands, e.g., halide ions) prefer square pyramidal structures and less polarisable ligands ( $\sigma$ -bonding ligands, e.g., NH<sub>3</sub>, H<sub>2</sub>O) lead to a irregular deformed coordination (coordination number 4 + 1 + 1) suggesting that the bonding effect of the ligands in the axial position cannot be ignored.

### Acknowledgement

Support by the *Österreichischer Fonds zur Förderung der Wissenschaftlichen Forschung* is gratefully acknowledged. We are indebted to Dr. C. Kratky for helpful discussions.

### References

- <sup>1</sup> Hathaway B. J., Billing D. E., *Coord. Chem. Rev.* **5**, 143 (1970).
- <sup>2</sup> Gazo J., Bersuker I. B., Garaj J., Kabesova M., Kohut J., Langfelderova H., Melnik M., Serator M., Valach F., *Coord. Chem. Rev.* **19**, 253 (1976).
- <sup>3</sup> Gagliardi E., Popitsch A., *Monatsh. Chem.* **103**, 1337 (1972).
- <sup>4</sup> Kratky C., Jorde C., Popitsch A., *Monatsh. Chem.* **113**, 933 (1982).
- <sup>5</sup> Kratky C., Jorde C., Popitsch A., *Monatsh. Chem.* **114**, 829 (1983).
- <sup>6</sup> Wendtland, W., *Thermal Methods of Analysis*, in: *Chemical Analysis*, Vol. **19**. New York: John Wiley. 1974.
- <sup>7</sup> Popitsch A., Gagliardi E., Schurz J., Kratky C., *Monatsh. Chem.* **112**, 537 (1981).
- <sup>8</sup> Nakamoto K., *Infrared and Raman Spectra of Inorganic and Coordination Compounds*. New York: John Wiley. 1978.
- <sup>9</sup> Scott K. L., Wieghardt K., Sykes A. G., *Inorg. Chem.* **12**, 655 (1973).
- <sup>10</sup> Schmidt K. H., Müller A., *Coord. Chem. Rev.* **19**, 41 (1976).
- <sup>11</sup> Anufrienko V. F., Mamaeva E. K., Rukhadze E. G., Ilina I. G., *Theor. Exp. Chem. Acad. Sci. Ukr. SSR* **3**, 204 (1967).